IOP Conf. Series: Earth and Environmental Science **163** (2018) 012020 doi:10.1088/1755-1315/163/1/012020

Improved Schnerr-Sauer cavitation model for unsteady cavitating flow on NACA66

X B ZHENG[1], L L LIU[1], P C GUO[1], F HONG[2] and X Q LUO[1]

[1] Institute of Water Resources and Hydro-electric Engineering, Xi'an University of Technology, Xi'an, China
[2] College of Mechanical and Power Engineering, Three Gorges University, Yichang, China

Email: lililiu2018@163.com

Abstract. For the purpose of comparing the capability for improved Schnerr-Sauer model, unsteady and turbulent cavitating flows over the three-dimensional NACA66 hydrofoil with fixed angle of attack of α=6° were numerically investigated based on Schnerr-Sauer (S-S) model and improved Schnerr-Sauer model, respectively. The SST *k-ω* model with local density correction was applied for the turbulence modeling and the effect of turbulence fluctuation was considered as well. Hydrodynamic coefficients, time-evolution of cloud cavity and the surface average pressure based on different cavitation models were obtained from simulations. in the stage of unsteady cavitation, the drag coefficient obtained from the improved S-S model close better with the value measured in experiment. The time-evolution of cloud cavity predicted by improved S-S model is much stronger and has better agreement with the experimental results as compared with the solution of S-S model.

1. Introduction

As cavitation generally occurs when the local fluid pressure reduces to the saturated vapor pressure and involves complex interaction between phase-change and vortex structures, the unsteady breakdown and shedding of the cavities will induce strong transient loads and lead to further hydrodynamic instabilities, even structure failures. Cavitation flow is a complex two phase flow, this process involves phase change、mass transport、fluid compressibility and unsteady flow.

In the past few decades, Leroux et al [1] investigated unsteady cavtitation flow on the NACA66 surface. The results showed that bubble collapse suddenly is due to the impact of pressure wave. Zhou et al [2] used the standard renormalization-group (RNG) turbulence model investigated the effect of non-condensable gas mass fraction in singhal model to hydrofoil cavitation.Zhang et al [3] used a dynamic cavitation model to simulated the pressure wave.of the hydrofoil surface. Huang et al [4] take the three-dimensional hydrofoil as objectives and proposed a dynamic non-linear subgrid model to investigated the unsteady partial/clould cavitating flows. Hong et al [5] raised a Filter-based density correction model (FBDCM) utilized for the turbulence modelling to investigated a 2-D Clark-Y hydrofoil, particular emphasis on understanding the effect of cavitation structures and the shedding dynamics on the hydrodynamics coefficients surrounding vortexs. In cavitating flow simulations, the turbulence model is crucial because the cavitation is basically unsteady in nature and there are strong interactions between the cavity interface and the boundary layer during cavity development. Though the current Reynolds average Navier–Stokes (RANS) equation approach has been widely used to

model turbulent flows in industry, the RANS models with eddy viscosity turbulence models have limited capability to simulate unsteady cavitating flows and need some modifications

In the present simulation, with the second development technique of CFX, the two default cavitating model in CFX is imported into the software by the CEL. In this paper, the modified SST k-ω turbulence model was utilized [9], and the effects of the turbulence kinetic energy of schner-sauer (SS) cavitation model and improved Schnerr-Sauer model was considered.

2. Governing equations and mathematical model

2.1. Schnerr-Sauer model

The cavitation model is carry through vapor phase and liquid phase interface to mass transfer, taken mixture of water and vapour as contain a large number of spherical vapour mixture, represent the process of evaporation and condensation respectively [8]:

$$R_e = \frac{\rho_v \rho_l \alpha_v (1-\alpha_v)}{\rho_m} \frac{3}{R_B} \sqrt{\frac{2(p_v - p)}{3\rho_l}} \tag{1}$$

$$R_c = -\frac{\rho_v \rho_l \alpha_v (1-\alpha_v)}{\rho_m} \frac{3}{R_B} \sqrt{\frac{2(p - p_v)}{3\rho_l}} \tag{2}$$

where α_v is local vapor void fraction, ρ_m is Mixed phase density and ρ_v is Vapor phase density

2.2 Improved Schnerr-Sauer model

The governing equations describe the cavitation process in-volving a two-phase and three-component system, where it is assumed that there is thermal equilibrium between all components and phases, and no-slip between any phases. The three components are respectively: Vapor (v), water (w) and non-condensable (g):

$$\frac{1}{\rho_m} = \frac{1 - f_g}{\alpha_v \rho_v + (1 - \alpha_v - \alpha_g)\rho_l} \tag{3}$$

Where α_g and f_g represent the volume fraction and mass fraction of noncondensable gas.

The improved Schnerr-Sauer model was [5]:

$$R_e = \frac{\rho_v \rho_l \alpha_v \left(1-\alpha_v - \alpha_g\right)}{\rho_m} \frac{3}{R_B} \sqrt{\frac{2\left(p_v - p\right)}{3\rho_l}} \tag{4}$$

$$R_c = -\frac{\rho_v \rho_l \alpha_v (1-\alpha_v - \alpha_g)}{\rho_m} \frac{3}{R_B} \sqrt{\frac{2(p - p_v)}{3\rho_l}} \tag{5}$$

2.3 Correction of turbulence model and numerical method

As mentioned in Ref [7], the widely used *k-ε* turbulence model cannot accurately predict the unsteady cavitating flow. The modified *SST* model is used as the turbulence model. The turbulent eddy viscosity μ_t is described as follows:

$$\mu_T = \frac{f(\rho_m)k}{\omega} / \max[\frac{1}{a^*}, \frac{SF_2}{a_1 \omega}] \tag{6}$$

$$f\left(p\right) = \rho_v + (1-\alpha_v)^n (\rho_l - \rho_v) \tag{7}$$

Where *n* is valued at 10, *k* and *ε r*epresent the turbulent kinetic energy and the dissipation rate.

3. Simulation setup

The time-dependent governing equations were discretized in both the space and time domains. The second order upwind scheme was used for the convective term, with the second order central difference scheme used for the diffusion term in the governing equations. The second-order implicit formulation was used for the transient term. The direct coupling method was used to solve the equations. The simulations were conducted using the CFD code ANSYS-CFX.

The unsteady cavitating flow simulations were started from a steady non-cavitating flow field. Then, the cavitation model and unsteady solver were turned on for the cavitating flow simulations. The time step was set to 1.407×10^{-4} s. The NACA66(mod) hydrofoil was used in the present research[1]. The hydrofoil has a relative maximum thickness of 0.12*c* at 0.45*c* chord length from the leading edge and a relative maximum camber of 2% at 50% from the leading edge. The hydrofoil chord length in the experiments was C=0.15 m and the foil was fixed within a 1 m long and 0.192 m wide square test section. The attack angle was 6 degrees. The inflow velocity was V_∞=5.33 m/s and the static pressure was assigned according to the cavitation number, which was defined as:

The computational domain is shown in Figure 1 as in the experiments, but a three-dimensional problem with 30 nodes in the spanwise direction. The hydrofoil was located in a channel having a height of 0.192 m. The domain inlet was 0.3 m upstream of the leading edge and the outlet was 0.90 m downstream of the leading edge. The boundary conditions had an imposed velocity at the inlet and a fixed static pressure at the outlet with free slip wall conditions at the upper and lower walls and non-slip walls on the hydrofoil. An O-H type grid was generated for the domain with sufficient refinement near the foil surface as shown in Figure 1. It is noted that the values of y+ calculated at the first grid point away from the hydrofoil surface were within 10. The present grid resolution was determined based on a grid dependence study with the final mesh having about 750710 nodes.

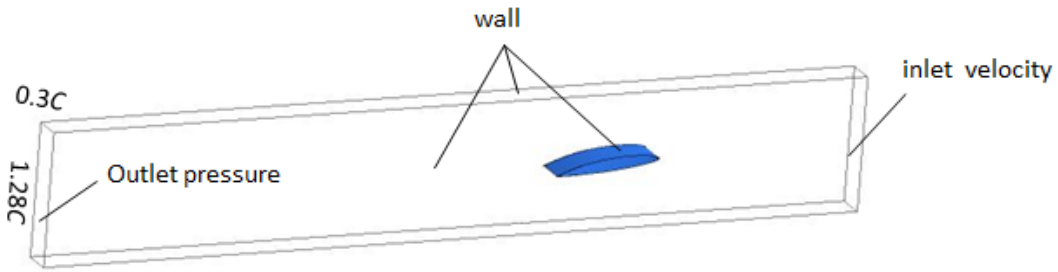

Figure 1 Computational domain and boundary conditions

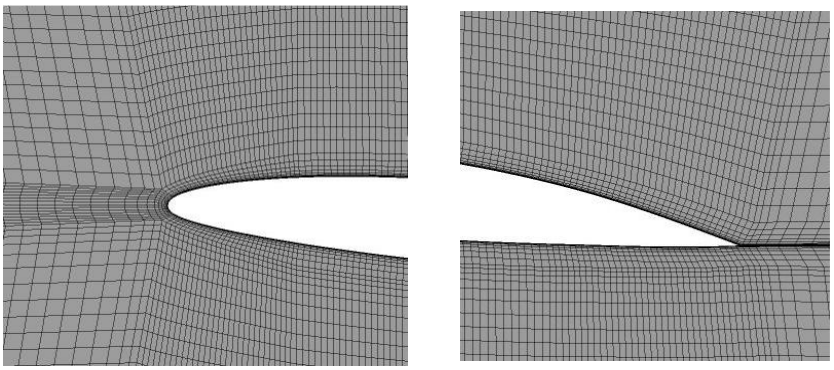

Figure 2 Close-up view of mesh near the leading edge (left) and the trailing edge (right) of the hydrofoil

4. Results and discussion

A typical unstable cloud cavitation occurred, when cavitation number drops to σ=1.25, At this stage, a large number of vortices shedding from the hydrofoil surface, and the load changes along the surface of the hydrofoil. The simulations in the present paper aim to analyze the unsteady cavitating flow characteristics of different cavitation models. The numerical results are compared with available experimental data [1] to analyze the capacity of cavitation model simulation unsteady cavitation.

Table 1 presents a comparison of average lift coefficient and the experiment using different cavitation model to simulation, it is noteworthy that the average lift coefficient *Cl*=0.943 by S-S model approximately the results of *Cl*=0.958 predicted by the improved S-S model, and the error were acceptable. The resistance coefficient error predicted by S-S is 14%, compared with the modified S-S model (error 2%), which shows that the improved cavitation model has better applicability to simulation unstable cavitation. It can also be found from the table that cavitation shedding frequency predicted by the improved S-S cavitation model is closest to the experimental.

Table 1. Comparisons of the time-averaged lift and drag coefficients predicted by different models

	Cl	Error/%	*Cd*	Error/%	*f/Hz*	Error/%
Exp	0.877	-	0.05	-	3.625	-
S-S model	0.943	7.53	0.057	14.00	3.215	11.313
Improved S-S model	0.958	9.21	0.049	2.00	3.886	7.20

Figure 3(a) shows the transient cavity patterns at six times by experimental observation [6], while those in figure 3(b) are the numerical results by the S-S model simulation and Figure 3(c) are the numerical results by the improved S-S model simulation These results show that: (i)The cavitation patterns and their evolution in one cycle predicted by the improved S-S model agree reasonably well with the experimental observations. The evolution of the cavitating flow in each cycle is very complicated and can be divided into the following steps. The first is the development of the attached cavity from the leading edge of the hydrofoil until the cavity grows to 50% of the chord length as shown in Figures 3(1/8T) -(3/8T). After the cavity grows more than half the chord length, the cavity shedding begins as shown in Figure 3(4/8T). As indicated in Figure 3(5/8T), the shedding cavity is rolled up and entrained downstream by the main flow. Finally, the vapor cloud collapses to downstream and a new attached sheet cavity appears at the leading edge. According to previous experimental observation, this cavity instability is due to the interaction between the cavity interface and the re-entrant flow at the rear part of the attached cavity. But S-S model predicted the cavitation development process was difference from the experimental observations, mainly to fall off in the hydrofoil trailing edge collapse bubble group, to continue the hydrofoil surface, the middle until the next cycle of cavitation to hydrofoil (*x/c*=0.5) before it disappeared.

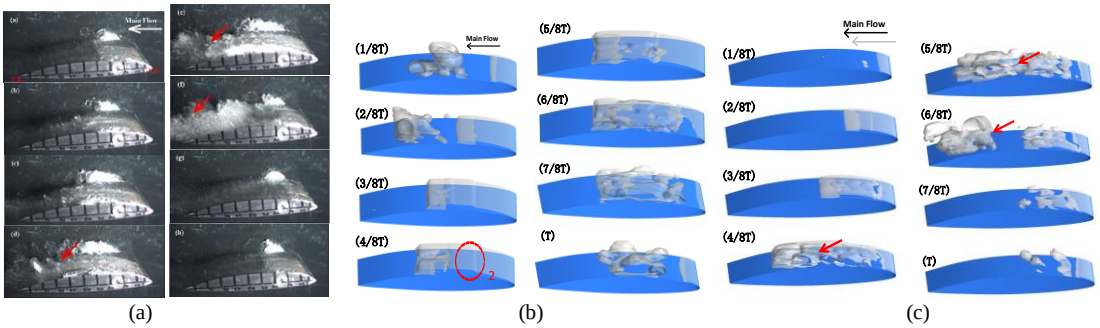

(a) (b) (c)

Figure.3. Time evolution of calculated cavitation shedding predicted by different cavitation models in one typical. (σ=1.25,α=6 deg).

In order to study the reasons for the difference evolution of the cavitating flow at the surface of the hydrofoil under different cavitation models, the pressure distribution along the suction surface of the chord length hydrofoil is obtained by numerical calculation, as shown in figure 4. We can see that the three predicted cavitation model to the hydrofoil suction surface average pressure coefficient in the x/c<0.22 (see figure 4(a)) in the region were higher than the experimental values, is mainly due to the reason of increased the pressure value. The average pressure coefficient predicted by the improved S-S model after 0.22c position agree with the experimental data best. It is worth noting that S-S model in x/c=0.41 (Figure 4(b)) at equal pressure coefficient and lower than the experimental values in Figure (3) find the cause, see figure 4(1 and 2) S-S model were produced at x/c=0.41 fold the sheet cavitation. The phenomenon reveals the close relationship between the evolution of cavitation and pressure.

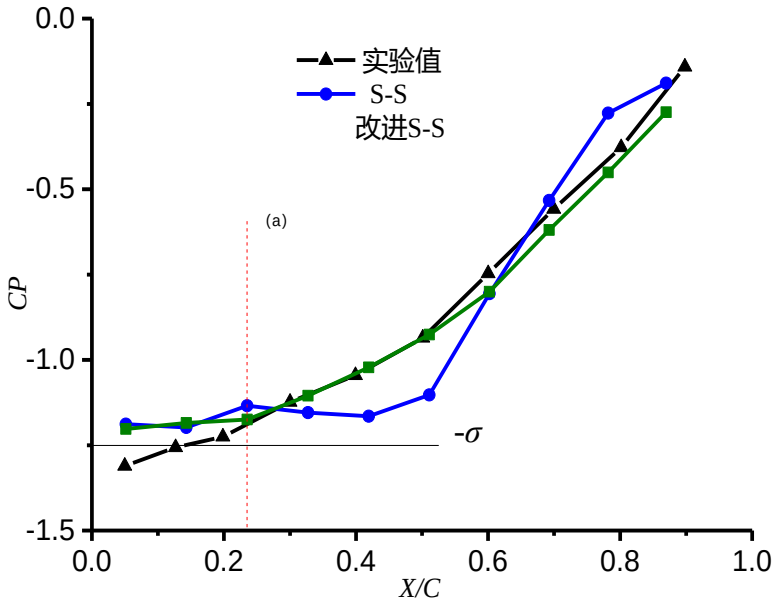

Figure.4. Average pressure coefficient distribution along hydrofoil surface calculated by different models

5.Conclusions

In the present paper,S-S model and improve S-S model simulations of unsteady cavitating flow around a NACA66 hydrofoil were performed. The numerical results were evaluated with experimental data to study the cavity evolution, shedding frequency and suction surface average pressure. Based on those results, the following conclusions can be drawn:

The simulation results of the S-S model and the modified S-S model show that the non-condensable gas had an important influence on the inception and development of cavitation and the quasi periodicity of cavitation The S-S model has a large error in predicted the hydrofoil surface drag coefficient, while the improved S-S model accurately predicted the hydrofoil surface drag coefficient.

The improved S-S model to accurately predicted unsteady cloud cavitation inception and development, collapse and sheding of the whole process, while the S-S model had shortcoming to simulation the unstable features.

The pressure coefficient of the suction surface simulation by improved S-S is basically consistent with the experiment since than x=0.22c. The pressure coefficient of the suction surface of the hydrofoil also revealed that cavitation evolution and pressure had a closed relationship.

Acknowledgement
This work was supported by the National Natural Science Foundation of China (Grant No. 51479166), the Key Research and Development Program of Shaanxi Province(Grant No. 2017ZDXM-GY-081) and the Scientific Research Program of Shaanxi Provincial Education Department (Grant No. 17JF019).

References

[1] Leroux J B, Astolfi J A, Billard J Y. An Experimental Study of Unsteady Partial Cavitation[J]. Journal of Fluids Engineering, 2004, 126(1):94-101.
[2] Zhou L, Zheng W W. Numerical Simulation of Cavitation Around a Hydrofoil and Evaluation of a RNG κ-ε Model[J]. Journal of Fluids Engineering, 2008, 130(1):011302-011308.
[3] X B ZHANG, W ZHANG, J CHEN Ye.Validation of dynamic cavitation model for unsteady cavitating flow on NACA66 [J]. Technological Sciences ,2014(4): 819-827.
[4] X b Huang, W Yang, Z q Liu. Study of unsteady cavitation on NACA66 hydrofoil using dynamic cubic nonlinear subgrid-scale model [J]. Mechanical Engineering , 2015, 7(11) .
[5] H Feng, Yuan J p, B l Zhou .Application of a new cavitation model for computations of unsteady turbulent cavitating flows around a hydrofoil [J]. Journal of Mechanical Science and Technology, 2017, 31 (1) 249~260.
[6] B Ji, X W Luo, Roger E.A. Arndt et al. Large Eddy Simulation and theoretical investigations of the transient cavitating vortical flow structure around a NACA66 hydrofoil[J]. International Journal of Multiphase Flow,2015,68 :121–134.
[7] Coutier-Delgosha O, Fortes-Patella R, Reboud J L. Evaluation of the Turbulence Model Influence on the Numerical Simulations of Unsteady Cavitation[C]// ASME Fedsm, June 2001, New Orleans. 2003:38-45.
[8] S J,Schnerr G H. Development of a new cavitation model based on bubble dynamics[J] . Journal of Applied Mathematics and Mechanics,2001,81(S3) : 561-562.
[9] B Ji, X WU Luo, Liu Y.,Xu H S, A Oshima. Numerical investigation of unsteady cavitating turbulent flow around a full scale marine propeller. [J]. Hydrodyn, 2010, 22 (5), 747e752.